

# Pressure-Driven Laminar Flow in Tangential Microchannels: an Elastomeric Microfluidic Switch

Rustem F. Ismagilov,<sup>†</sup> David Rosmarin,<sup>†</sup> Paul J. A. Kenis,<sup>†,§</sup> Daniel T. Chiu,<sup>†</sup> Wendy Zhang,<sup>‡</sup> Howard A. Stone,<sup>‡</sup> and George M. Whitesides<sup>\*,†</sup>

Department of Chemistry and Chemical Biology, Harvard University, Cambridge, Massachusetts 02138, and Division of Engineering and Applied Sciences, Harvard University, Cambridge, Massachusetts 02138

**This paper describes laminar fluid flow through a three-dimensional elastomeric microstructure formed by two microfluidic channels, fabricated in layers that contact one another face-to-face (typically at a 90° angle), with the fluid flows in tangential contact. There are two ways to control fluid flow through these tangentially connected microchannels. First, the flow profiles through the crossings are sensitive to the aspect ratio of the channels; the flow can be controlled by applying external pressure and changing this aspect ratio. Second, the flow direction of an individual laminar stream in multiphase laminar flow depends on the lateral position of the stream within the channel; this position can be controlled by injecting additional streams of fluid into the channel. We describe two microfluidic switches based on these two ways for controlling fluid flow through tangential microchannels and present theoretical arguments that explain the observed dependence of the flow profiles on the aspect ratio of the channels.**

This paper describes pressure-driven laminar flow through a simple three-dimensional structure composed of tangential microchannels ( $\mu\text{C}$ ) that cross at an angle of  $\sim 90^\circ$ , that is, perpendicular microfluidic channels that are in contact over a small area (Figure 1a). It is likely that future microfluidic channel systems will be three-dimensional and will be fabricated in multiple layers with channels that belong to different layers crossing over one another.<sup>1–3</sup> We are interested in using these crossings as nodes at which to control fluid flow. In particular, we want to direct flow from the channels of one layer to the channels of other layers. In this paper, we describe steady fluid flow through the contact area of two microchannels that cross tangentially at an angle of  $\sim 90^\circ$  (tangentially crossing microchannels,  $\mu\text{C}$ , Figure 1a). We find that the direction of flow of a laminar stream through  $\mu\text{C}$

strongly depends on the aspect ratio of the channels and on the position of this stream in the channel. We present theoretical arguments that explain the observed dependence of the flow on the aspect ratio, and use  $\mu\text{C}$  to construct microfluidic switches.

**Laminar Flow and the Reynolds Number.** The Reynolds number,  $Re$ , measures the relative influence of viscous and inertial effects in fluid flow and is a measure of the tendency of flow to become turbulent.<sup>4,5</sup> The Reynolds number is defined as the ratio of inertial forces to viscous forces and is dimensionless:  $Re = ul\rho/\mu$  where  $u$  is the average velocity of the flow (in m/s),  $l$  is the diameter of the channel (in m),  $\rho$  is the density (in kg/m<sup>3</sup>) of the fluid, and  $\mu$  is its shear viscosity (in kg/ms). For flow in a circular pipe, turbulence typically develops at  $Re > 2000$ .<sup>5</sup> Fluid flow in microfluidic systems is characterized by a low Reynolds number ( $< 100$ ) and is laminar. In contrast to turbulent flow, for laminar flow several streams of fluids in a capillary can flow in parallel without significant mixing; mixing occurs only by molecular diffusion. Yager et al. have used this feature of laminar flow to perform separation and detection of diffusing analytes in the adjacent fluid streams in a microchannel.<sup>6,7</sup> We have used laminar flow to perform spatially resolved surface chemistry and microfabrication inside microfluidic channels<sup>8,9</sup> and to pattern cells and their environments.<sup>10</sup> These and other applications of microfluidic systems rely on techniques for controlling low-Reynolds number fluid flows. Such flows can be controlled directly by controlling the geometry of the microfluidic network.<sup>11</sup> Microfluidic systems fabricated from elastomers appear especially attractive in this respect because their geometry can be changed in real time by applying external pressure.<sup>12,13</sup> Alternative methods of controlling

(4) Whitesides, G. M.; Stroock, A. D. *Phys. Today* **2001**, *54*, 42–48.

(5) Bird, R. B.; Stewart, W. E.; Lightfoot, E. N. *Transport Phenomena*; Wiley: New York, 1960.

(6) Weigl, B. H.; Yager, P. *Science* **1999**, *283*, 346–347.

(7) Kamholz, A. E.; Weigl, B. H.; Finlayson, B. A.; Yager, P. *Anal. Chem.* **1999**, *71*, 5340–5347.

(8) Kenis, P. J. A.; Ismagilov, R. F.; Whitesides, G. M. *Science* **1999**, *285*, 83–85.

(9) Ismagilov, R. F.; Stroock, A. D.; Kenis, P. J. A.; Whitesides, G.; Stone, H. A. *Appl. Phys. Lett.* **2000**, *76*, 2376–2378.

(10) Takayama, S.; McDonald, J. C.; Ostuni, E.; Liang, M. N.; Kenis, P. J. A.; Ismagilov, R. F.; Whitesides, G. M. *Proc. Natl. Acad. Sci. U.S.A.* **1999**, *96*, 5545–5548.

(11) Beebe, D. J.; Moore, J. S.; Yu, Q.; Liu, R. H.; Kraft, M. L.; Jo, B. H.; Devadoss, C. *Proc. Natl. Acad. Sci. U.S.A.* **2000**, *97*, 13488–13493.

(12) Unger, M. A.; Chou, H. P.; Thorsen, T.; Scherer, A.; Quake, S. R. *Science* **2000**, *288*, 113–116.

<sup>†</sup> Department of Chemistry and Chemical Biology.

<sup>‡</sup> Division of Engineering and Applied Sciences.

<sup>§</sup> Current Address: Department of Chemical Engineering, University of Illinois at Urbana-Champaign, Urbana, IL 61801

(1) Anderson, J. R.; Chiu, D. T.; Jackman, R. J.; Cherniavskaya, O.; McDonald, J. C.; Wu, H. K.; Whitesides, S. H.; Whitesides, G. M. *Anal. Chem.* **2000**, *72*, 3158–3164.

(2) Liu, R. H.; Stremmer, M. A.; Sharp, K. V.; Olsen, M. G.; Santiago, J. G.; Adrian, R. J.; Aref, H.; Beebe, D. J. *J. Microelectromech. Syst.* **2000**, *9*, 190–197.

(3) Jo, B. H.; Van Lerberghe, L. M.; Motsegood, K. M.; Beebe, D. J. *J. Microelectromech. Syst.* **2000**, *9*, 76–81.

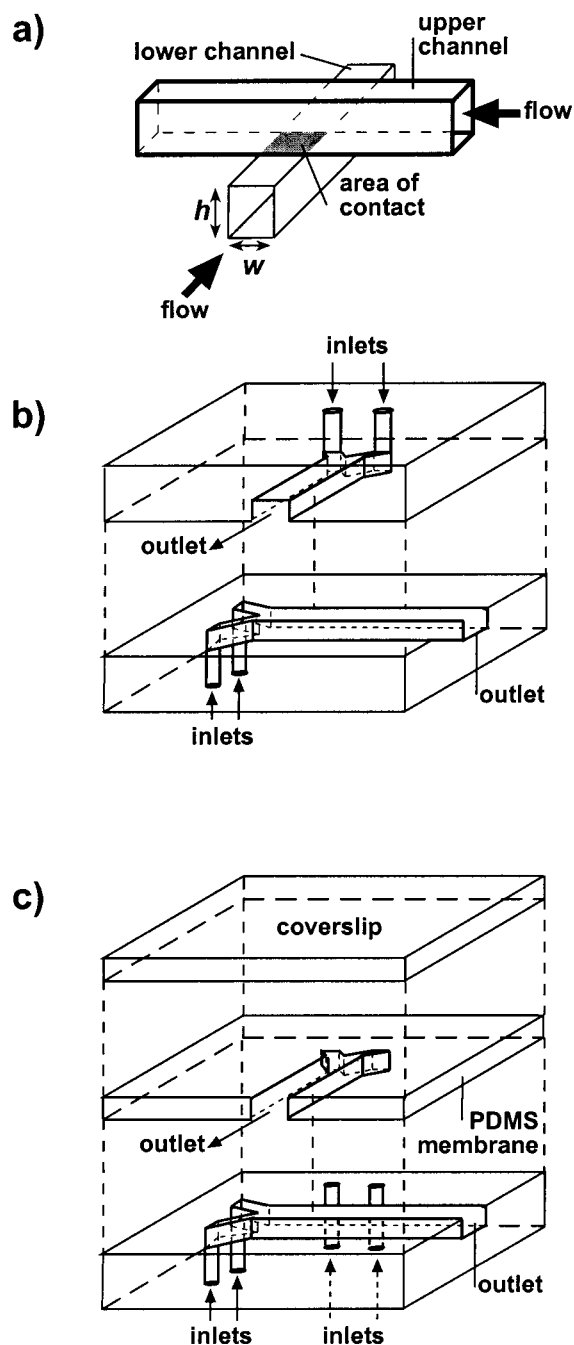


Figure 1. (a) Schematic drawing of the tangential microchannels ( $\mu\text{C}$ ) described in this paper. The typical dimensions are height of the channels,  $h$ , 20–200  $\mu\text{m}$ ; width of the channels,  $w$ , 100–400  $\mu\text{m}$ . The channels can exchange fluid through the shaded area of contact. (b) Fabrication scheme for  $\mu\text{C}$ . The inlets were fabricated simply by punching holes in PDMS. (c) Fabrication scheme for a device assembled on a thin glass cover slip and used for confocal visualization of flow patterns through  $\mu\text{C}$ .

and switching flows in microchannels include the use of electroosmotic flow,<sup>14,15</sup> thermally formed microbubbles,<sup>16</sup> and hydrogels.<sup>17</sup>

## EXPERIMENTAL SECTION

**Fabrication.** The fabrication of microfluidic systems in poly(dimethylsiloxane) (PDMS) is straightforward.<sup>1,18,19</sup> All of the devices described in this paper were fabricated in several layers. Sealing of these layers was accomplished by bringing into con-

tact pieces that had been briefly oxidized in an air plasma (approximately 1 min). A two-layer microfluidic system with tangential microchannels was fabricated by sealing two indistinguishable PDMS slabs, each bearing one channel structure, face to face (Figure 1b). To ensure that the channels are perpendicular and symmetric about the crossing, we used alignment marks on the PDMS slabs and used an alignment procedure described previously.<sup>1</sup> The device used for confocal visualization was fabricated in a different fashion (Figure 1c). A PDMS membrane containing the channel structure as a trench with vertical side walls, open on top and bottom, was prepared; the thickness of the membrane (and the height of the channel) was 40  $\mu\text{m}$ . A slab of PDMS (4–5 mm thick) bearing a similar channel structure was sealed to one side of this membrane, and a glass cover slip (no. 1,  $\approx 130 \mu\text{m}$  thick) was sealed to the other side. Access holes were punched through the thicker slab of PDMS using a 21-gauge syringe needle that had been cut to remove its slanted tip, polished, and then sharpened. In this paper we consider only tangential microchannels that cross at right angles, although we have observed similar behavior at other crossing angles (45° to 135°). Typical microchannels were 100 or 400  $\mu\text{m}$  wide,<sup>20</sup> 25–200  $\mu\text{m}$  high, and 2–4 cm long.

**Experimental Method.** All of the experiments were conducted with pressure-driven flow generated by a syringe pump (Orion). Disposable syringes (1 mL) with 27-gauge needles were connected to the microfluidics device with polyethylene tubing (i.d. = 0.38 mm, o.d. = 1.09 mm). Volumetric flow rates were controlled by the settings of the syringe pump; these settings were adjusted for devices of different aspect ratios to produce flows having the same Reynolds number value. The flow patterns were visualized using filtered aqueous solutions of commercially available aqueous inks (Watermark). Three-dimensional flow profiles were visualized with a Leica confocal microscope.

The flow patterns were quantified by labeling the fluid entering one of the two microchannels with a red dye ferriin (1,10-phenanthroline iron(II) sulfate complex). Fluid exiting from the microfluidic system was allowed to flush the tubing that connected the microfluidic system to a reservoir for sample collection for 1–5 min. Samples (200–300  $\mu\text{L}$ ) of this fluid were collected, and their optical densities were measured using a diode array UV–vis spectrophotometer (Hewlett-Packard) at the absorption maximum of ferriin (510 nm). We checked that the flows through the two microchannels are symmetric in two ways: (i) we made

- (13) Young, A. M.; Bloomstein, T. M.; Palmacci, S. T. *J. Biomech. Eng.-Trans. ASME* **1999**, *121*, 2–6.
- (14) Duffy, D. C.; Schueller, O. J. A.; Brittain, S. T.; Whitesides, G. M. *J. Micromech. Microeng.* **1999**, *9*, 211–217.
- (15) Schasfoort, R. B. M.; Schlautmann, S.; Hendrikse, L.; van den Berg, A. *Science* **1999**, *286*, 942–945.
- (16) Lin, L. W. *Microscale Thermophys. Eng.* **1998**, *2*, 71–85.
- (17) Beebe, D. J.; Moore, J. S.; Bauer, J. M.; Yu, Q.; Liu, R. H.; Devadoss, C.; Jo, B. H. *Nature* **2000**, *404*, 588–590.
- (18) Duffy, D. C.; McDonald, J. C.; Schueller, O. J. A.; Whitesides, G. M. *Anal. Chem.* **1998**, *70*, 4974–4984.
- (19) McDonald, J. C.; Duffy, D. C.; Anderson, J. R.; Chiu, D. T.; Wu, H. K.; Schueller, O. J. A.; Whitesides, G. M. *Electrophoresis* **2000**, *21*, 27–40.
- (20) The pressure drop required to pump fluids through a channel of a low aspect ratio increases as the inverse third power of the height of the channel. We observed that at higher flow rates (30  $\mu\text{L}/\text{min}$ ), elastomeric PDMS channels of height = 5  $\mu\text{m}$  distorted due to excessive pressures. We did not observe this distortion for channels of height = 20–25  $\mu\text{m}$ , and therefore, we chose to use these higher (and proportionally wider) channels for our low-aspect ratio measurements.

sure that the volumes of the fluid exiting from the two channels were the same and (ii) after the data were collected, we switched the fluids (water and solution of ferroin) in the two channels and repeated the experiment.

## RESULTS AND DISCUSSION

**Influence of the Aspect Ratio of the Channels.** The flow pattern at the crossing of tangential microchannels is independent of the contact area between them<sup>21</sup> and strongly depends on their aspect ratio,  $A$ , defined as the ratio of the height,  $h$ , to the width,  $w$ , of the channels ( $A = h/w$ , Figure 1a). When the aspect ratio is high (e.g.,  $A = 1.6$ ), the fluids continue straight through the crossing without significant exchange of fluid between the channels (Figure 2a). When the aspect ratio is low (e.g.  $A = 0.058$ ), most of the fluid turns from one channel into another (Figure 2c). It was this exchange of fluid between the two tangential microchannels that we wanted to quantify and use.

To illustrate the three-dimensional flow profile, we used fluorescence confocal microscopy. We obtained the image shown in Figure 2d by flowing water into the top channel and a solution of fluorescein into the bottom channel and taking a confocal cross section of fluorescence at the exit of the top channel.<sup>22</sup> Qualitatively, this image can be interpreted by regarding the flow in each channel composed of an array of laminar streams. After entering the crossing, such laminar streams exit the crossing through the outlet nearest to the point of entry, traveling the shortest possible distance. For example, fluorescently labeled streams on the top of the lower channel in Figure 2d exit by turning into the bottom of the upper channel, the nearest outlet for those streams. Fluorescently labeled streams on the bottom of the lower channel exit by continuing straight through the lower channel, their nearest outlet. To turn, a fluid stream has to travel a distance determined primarily by the height of the channel,  $h$ , whereas to continue straight, a fluid stream has to travel a distance determined primarily by the width of the channel,  $w$ . Because of this interplay between  $h$  and  $w$ , the overall flow behavior depends on the aspect ratio of the channels, as quantified below.

**Quantitative Analysis of the Flow Patterns.** To quantify the flow through  $\mu\text{C}$ , we calculated normalized quantities,  $Q_S$  (volumetric flow rate of the fluid continuing straight through the crossing) and  $Q_T$  (volumetric flow rate of the fluid turning at the crossing), in which we normalized the total flow rate of fluid entering through one channel and exiting through both channels to the value of 1 so that  $Q_S + Q_T = 1$ . To quantify the fluid exchange between the channels experimentally, we labeled the flows in them. In one channel, we used an aqueous solution of ferroin with known optical density; in the other, we used water (experiment as in Figure 2). The typical velocity through the

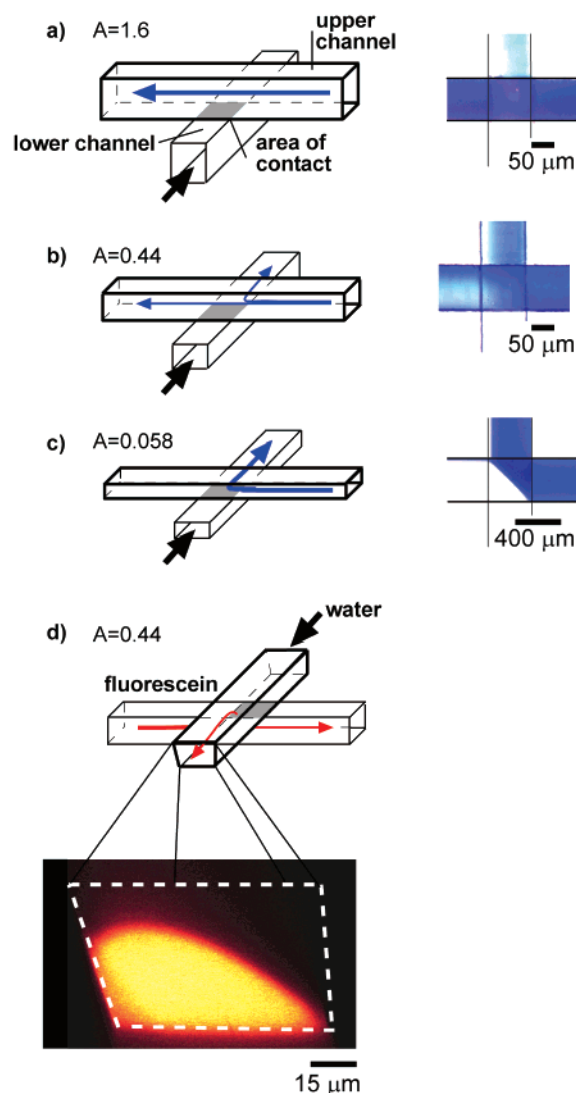


Figure 2. (a–c) Schematic drawings (left column) and top view microphotographs (right column) of laminar flow at  $Re = 10$  through  $\mu\text{C}$  (width,  $\mu\text{m} \times$  height,  $\mu\text{m}$ ) of different aspect ratios  $A$ . (a)  $100 \times 160$ ,  $A = 1.6$ ,  $Q_S = 0.96$ ; (b)  $100 \times 44$ ,  $A = 0.44$ ,  $Q_S = 0.47$ ; (c)  $400 \times 23$ ,  $A = 0.058$ ,  $Q_S = 0.026$ . (d) Fluorescent confocal image illustrating three-dimensional flow profile of the fluid exiting the crossing of  $\mu\text{C}$  with  $A = 0.44$  (as in b).<sup>22</sup> In this experiment, fluorescein was entering  $\mu\text{C}$  through the bottom channel and water was entering through the top channel. Fluorescence observed in the top channel corresponds to the labeled fluid turning from the bottom channel into the top channel. This fluorescence was visualized by confocal microscopy; a vertical confocal slice through the top channel was taken downstream from the crossing. Bright yellow regions correspond to the stream carrying fluorescein, and it is surrounded by red areas that arise as a result of imperfect confocality of the instrument. The viewing direction for the image is opposite to the flow direction. The method of assembly of the channel system that was used (Figure 1c) distorted the walls of the lower channel, and the upper channel is trapezoidal in cross section rather than rectangular.

channel was  $10 \text{ cm/s}$ , corresponding to  $1 \text{ ms}$  contact time between two crossing streams in a  $100 \mu\text{m}$ -wide channel. Therefore, the diffusion of ferroin between two streams continuing straight through the channels is negligible on the time scales of interest; the ratio  $Q_S/Q_T$ , therefore, equals the ratio of the optical density of the fluid collected from the channel into which the solution of ferroin was allowed to flow to the optical density of the fluid

(21) We found that different contact areas of crossing channels with the same aspect ratios give results that are the same within the experimental error. For example, in the graph shown in Figure 3b, the third data point from the left ( $w = 400 \mu\text{m}$ ,  $h = 84 \mu\text{m}$ ,  $A = 0.21$ ,  $\log(A) = -0.68$ ) and the fourth data point from the left ( $w = 100 \mu\text{m}$ ,  $h = 25 \mu\text{m}$ ,  $A = 0.25$ ,  $\log(A) = -0.60$ ) are in excellent agreement with each other and the rest of the data.

(22) We determined the cross-sectional shape of the channel shown in Figure 2d (white dashed line) by confocal imaging of the channel completely filled with fluorescein. This cross section is not rectangular as a result of the distortion of the thin PDMS membrane ( $40 \mu\text{m}$ ) used as the middle layer in the fabrication of the device. The devices used for quantitative measurements were made out of thick PDMS slabs ( $4\text{--}5 \text{ mm}$ ) and were not distorted.

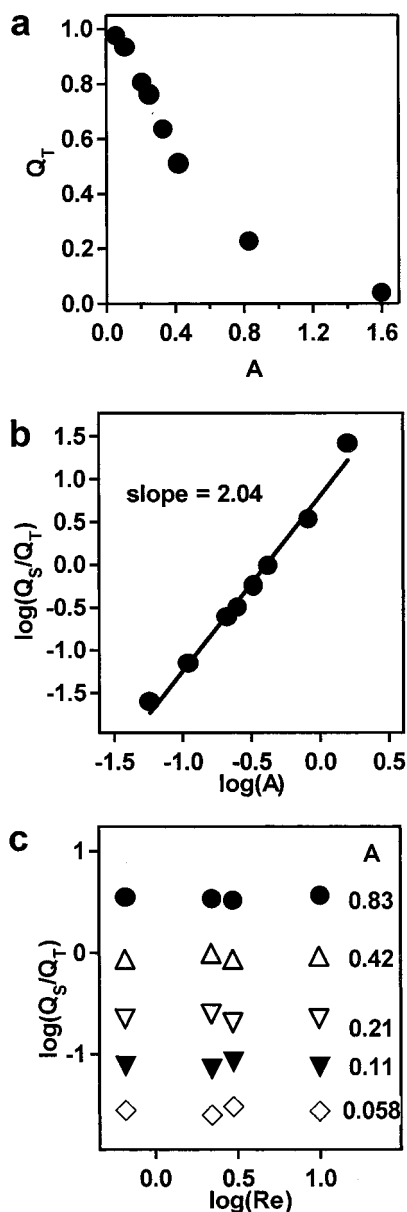


Figure 3. Quantitative data that correspond to the experiment described in Figure 2.  $A$  is the aspect ratio of the channels,  $Q_T$  is the fraction of the colored fluid that is turning (that is, injected from one channel into the other channel), and  $Q_S$  is the fraction of the colored fluid continuing straight (that is, remaining in the same channel). (a) Fraction of the fluid turning as a function of the aspect ratio of the channels at  $Re = 2.5$ . (b) Logarithmic plot of  $Q_S/Q_T$  as a function of the aspect ratio at  $Re = 2.5$ . (c) Logarithmic plot of  $Q_S/Q_T$  as a function of  $Re$  demonstrating negligible dependence on  $Re$ . For all of the plots, the error bars are the size of the symbols.

collected from the other channel (Figure 3a). For channels with a high aspect ratio ( $A > 1.4$ ) we measured  $Q_S > 0.9$ ,  $Q_T < 0.1$ ; for channels with low aspect ratio ( $A < 0.1$ ) we measured  $Q_S < 0.1$ ,  $Q_T > 0.9$ . These measurements are consistent with the images shown in Figure 2. A plot of  $\log(Q_S/Q_T)$  versus  $\log A$  is linear with a slope of approximately 2 (Figure 3b). This power-law dependence is rationalized below.

**Theory of Flow-Through  $\mu$ c.** Here we sketch a qualitative physical explanation for flows through tangential microchannels. We emphasize that the observed dependence of the flow patterns on the channel aspect ratio arises solely from the fact that the

channels are stacked on top of each other in direct contact.<sup>23</sup> The applied pressure gradient drives a flow against viscous resistance from the channel walls, and the inertial effects associated with these flows are negligible, because the flows are steady and in the laminar regime ( $Re \leq 10$ ). A fluid element at the junction of  $\mu$ c has two choices: (i) going straight by moving through a rectangular cross section of area  $h \times w$ , and exiting through the channel from which it entered the junction or (ii) turning by moving through the contact area  $w \times w$  between the two channels and exiting through the perpendicular channel. If the aspect ratio  $A$  is small ( $h \ll w$ ), then there is less resistance for the fluid to flow through the contact area between the two channels ( $w \times w$ ) and turn than to continue straight. If the aspect ratio is large ( $h \gg w$ ), then there is less resistance for the fluid to flow straight through the larger cross section ( $h \times w$ ) of the channel than there is to turn by moving through the smaller contact area ( $w \times w$ ). This qualitative discussion is consistent with the flow patterns shown in Figure 2.

In the laminar flow regime, the pressure gradient,  $G$  (in Pa/m), required to achieve an average velocity,  $u$ , through a channel is described by  $G \approx \mu u/P$ , in which  $l$  (in m) is a typical lateral dimension of the channel. We define  $G_S$  to be the pressure gradient associated with the fluid flowing straight through the junction, and  $G_T$  to be the pressure gradient associated with the fluid flowing upward or downward from one channel into the other. For a channel of rectangular cross section with small aspect ratio ( $h \ll w$ ),  $l$  corresponds to the smaller dimension  $h$  (the height of the channel), because the largest pressure gradient is associated with forcing the fluid to flow through closely spaced top and bottom channel walls, and  $G_S \approx \mu u/h^2$ . On the other hand,  $G_T \approx \mu u/w^2$ , because the pressure gradient associated with turning is roughly the pressure gradient due to upward or downward flow through the contact area ( $w \times w$ ) between the two channels. Therefore,  $G_T/G_S \approx (h/w)^2$ , and we see that when the aspect ratio  $h/w$  is small,  $G_T$  is much smaller than  $G_S$ . In these conditions, there is less resistance for the fluid to turn than to go straight through the junction. Because the flows are at low Reynolds numbers, the normalized volumetric flow rates associated with the flows continuing straight ( $Q_S$ ) and turning ( $Q_T$ ) can be written as a function of the ratio of pressure gradients  $G_T/G_S$ :  $Q_S = f(x)$  and  $Q_T = [1 - f(x)]$ , where  $x = G_T/G_S$ . We are most interested in  $x = G_T/G_S \ll 1$ . By definition,  $Q_S + Q_T = 1$ , and therefore,  $f(x)$  varies from 0 to 1. The low-aspect ratio limit corresponds to the limit  $G_T/G_S \rightarrow 0$ , and therefore,  $x \rightarrow 0$ . In this limit,  $f(x)$  has the Taylor expansion  $f(x) = f(0) + f'(0)x + \dots$ , where  $f' = df/dx$ . We then write  $Q_S/Q_T$  in terms of  $f(x)$  and expand  $f(x)$  into the Taylor expansion. Because  $f(0) = 0$ , we have  $Q_S/Q_T \approx f'(0)x/[1 - f'(0)x] \approx f'(0)x$  (because  $x \rightarrow 0$ ). Because  $f'(0)$  is a constant, we have  $Q_S/Q_T \propto x = G_T/G_S = (h/w)^2 = A^2$ . This dependence on the aspect ratio ( $Q_S/Q_T \propto A^2$ ) is observed in the experiments (Figure 3b). Additional experiments performed over a range of Reynolds numbers demonstrate that below  $Re = 10$ , the results are independent of the Reynolds number within the experimental uncertainty (Figure 3c), because the flow in the  $\mu$ c has remained laminar in all of the experiments.

(23) In contrast to the results presented here for tangential microchannels, flow patterns through crossings of in-plane channels do not depend on the aspect ratio of the channels.

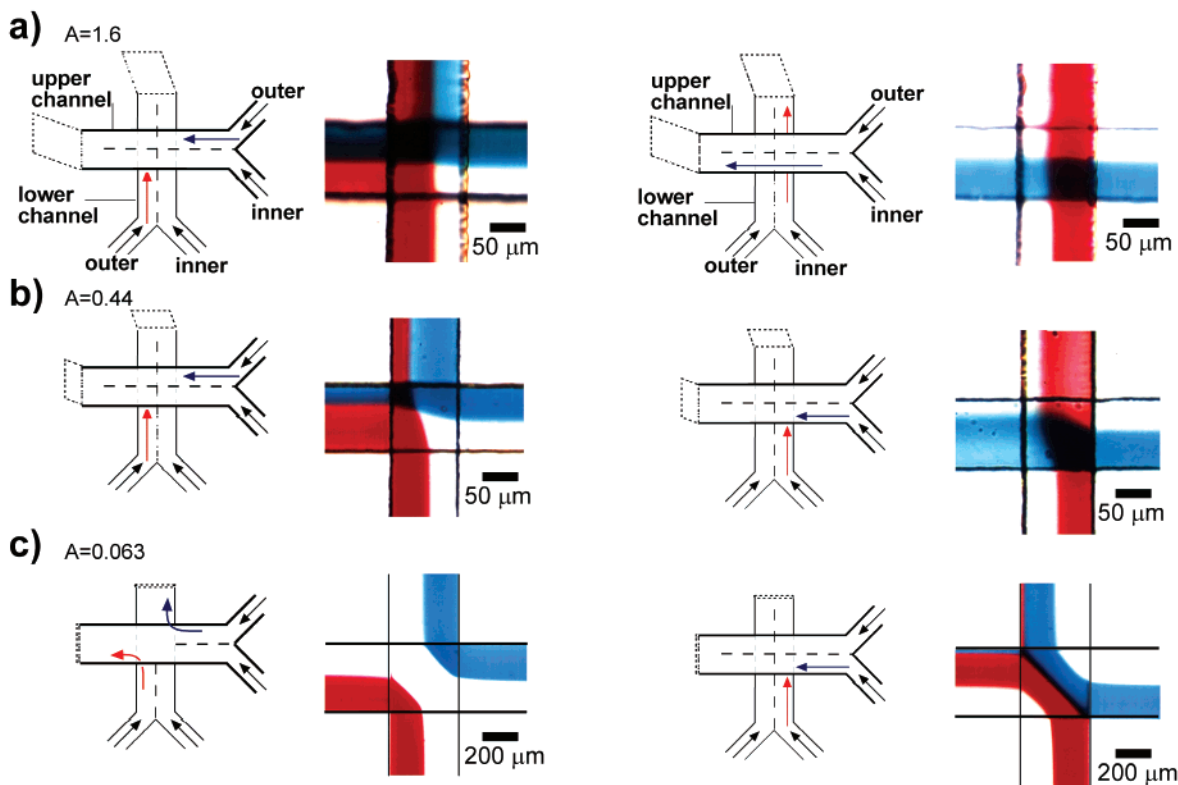


Figure 4. Two-stream laminar flow at  $Re = 10$  through  $\mu c$  (width,  $\mu m \times$  height,  $\mu m$ ) of different aspect ratios  $A$ . (a)  $100 \times 160$ ,  $A = 1.6$ ; (b)  $100 \times 44$ ,  $A = 0.44$ ; (c)  $400 \times 25$ ,  $A = 0.063$ .

**Multiphase Laminar Flow through the Crossing.** To simplify the discussion, we consider the flow in each channel to comprise multiple parallel laminar streams. We used multiphase laminar flow to show that for  $\mu c$  of a given aspect ratio, the flow direction of a laminar stream depends predictably on its position within the channel (Figure 4). The outer streams (those closer to the outlet of the crossing channel) have a greater tendency to turn than do the inner streams (those closer to the inlet of the crossing channel). We can take advantage of this dependence and use multiphase laminar flow to control fluid flow through  $\mu c$ . For the channels of high aspect ratio (Figure 4a), we can increase the fraction of the colored fluid that goes straight through the crossing by placing this fluid in the inner streams (labeled "inner" in Figure 4a). For the channels of low aspect ratio (Figure 4b), we can enforce complete turning of the colored fluid by placing it in the outer streams. In addition, for channels of intermediate aspect ratios (Figure 4c), we can switch the direction of the flow of a particular stream by switching its position from inner (the stream will continue straight) to outer (the stream will turn). A switch based on this phenomenon is described below.

**Application to Microfluidic Systems: Switching by Controlling the Position of the Stream in the Channel.** Figure 5 shows a switch that operates by using multiphase laminar flow to control the position of the input streams within each of the channels. Each of the channels has three inlets, two of which are used at any time. Aqueous solutions of interest (dyed red or green) are injected through the middle pair of inlets. Water is injected through either the outer or the inner pairs of inlets (see Figure 4 for the nomenclature) in order to focus the width of the colored streams to approximately one-sixth of the width of the channel

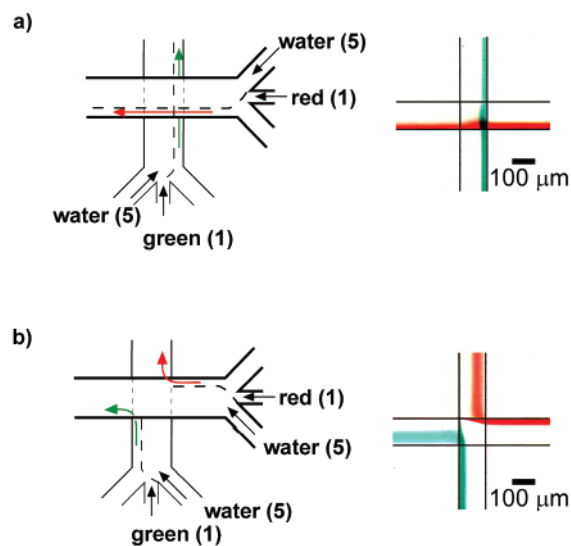


Figure 5. A fluidic switch based on  $\mu c$ . Switching is accomplished by controlling the position of the colored stream in the channel by applying pressure of water from the side inlets of each channel.

and to position these streams within the channel. When water is injected through the outer inlets, the colored fluid continues straight through the crossing region (Figure 5a). When water is injected through the inner inlets, the colored fluid occupies the outer part of the channel and turns (Figure 5b).

**Application to Microfluidic Systems: Switching by Changing the Aspect Ratio of the Channel.** Figure 6 shows a microfluidic switch that takes advantage of multiphase laminar flow and the elastomeric properties of the systems of  $\mu c$ . To change the aspect ratio of  $\mu c$ , we used the pneumatic actuation

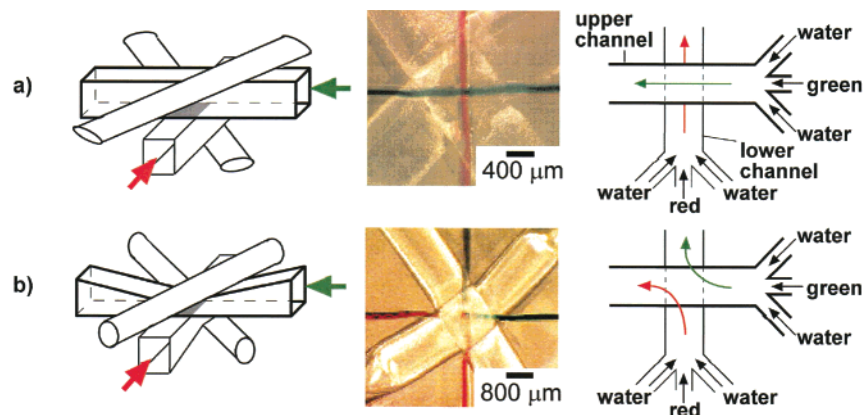


Figure 6. An elastomeric microfluidic switch based on the tangential microchannels. In this system, pieces of elastic tubing were molded above and below the crossing of  $t_{\mu c}$  of high aspect ratio ( $A = 1.2$ ). The green and red dye were localized in the centers of the channels by streams of water from the side inlets. (a) Fluid flows straight through  $t_{\mu c}$  of high-aspect ratio. (b) When pressure of air is applied to the elastic tubing, the tubing expands and squeezes the channels, decreasing their aspect ratio and forcing the marked streams of fluid to turn and switch channels.

approach described by Quake et al.<sup>12</sup> We modified the  $t_{\mu c}$  system by molding PDMS tubes (Silastic brand) above and below the crossing of  $t_{\mu c}$  ( $w \times h = 200 \mu\text{m} \times 240 \mu\text{m}$ ). At the crossing, fluid was localized in the centers of the channels by flow of water from side inlets and continued straight through these high aspect ratio channels (Figure 6a). The direction of flow was reversibly switched by pressurizing PDMS tubing with air (2 atm). The expanded PDMS tubing squeezed the channels, decreased their aspect ratio (Figure 6b), and caused the flows to turn. The data in Figure 3 could be used to control the response of this switch quantitatively.

## CONCLUSION

Crossing channels can be used to control fluid flow, that is, to direct flow from channels of one layer of a microfluidic system to the channels of another layer. In this system, the flow path of a laminar stream of fluid within the channel is sensitive to both the lateral position of the stream in the channel and the aspect ratio of the channel. Multiphase laminar flow allows the direction of the streams to be switched by controlling their lateral position. The fact that PDMS is an elastomer allows us to change the aspect ratio of the channels by applying external pressure and, thus, to control the flow actively. The systems described in this paper have

no hinges or other parts that require surfaces to move against one another; they may find applications as microfluidic switches. They would seem especially useful for fluids containing suspended particulates that might jam conventional valves or fluids that contain delicate biological samples, such as mammalian cells. The observed flow patterns can be rationalized by considering the pressure gradients at the crossing of tangential microchannels.

Elastomeric microfluidic structures with externally reconfigurable geometries<sup>11</sup> are interesting, because they may be designed to take advantage of both the stability of laminar flow and the sensitivity<sup>2</sup> of laminar flow to geometry. These structures, such as the tangential microchannels described in this paper, may allow new forms of control of fluid flow that have no analogues in macroscopic fluidic systems in which flow is dominated by turbulence.

## ACKNOWLEDGMENT

This work was supported by DARPA and NSF ECS-0004030 and ECS-9729405. We thank Jacqueline Ashmore (Harvard) for helpful discussions.

Received for review April 2, 2001. Accepted July 8, 2001.

AC010374Q